research

DTIC FILE COPY

report no. FEL-89-B336

copy no. 7

Measurement results of the FEL-TNO planar rectangular near field facility (1978-1989)

AD-A225 065

TDCK
Postbus 90701 2509 LS 's-Gravenhage

DTIC
ELECTE
AUG 07 1990
S C E D

DISTRIBUTION STATEMENT A
Approved for public release;
Distribution Unlimited

90 08 03 043

Netherlands
organization for
applied scientific
research

TNO-report

TNO Physics and Electronics
Laboratory

P.O. Box 96864
2509 JG The Hague
Oude Waalsdorperweg 63
The Hague, The Netherlands

Phone +31 70 26 42 21

report no. FEL-89-B336

copy no. 7

title

Measurement results of the FEL-TNO planar rectangular near field facility (1978-1989)

Nothing from this issue may be reproduced and/or published by print, photoprint, microfilm or any other means without previous written consent from TNO. Submitting the report for inspection to parties directly interested is permitted.

In case this report was drafted under instruction, the rights and obligations of contracting parties are subject to either the 'Standard Conditions for Research Instructions given to TNO' or the relevant agreement concluded between the co-acting parties on account of the research object involved.

© TNO

author(s):

Ir. J.G. van Hezewijk

QUALITY INSPECTED 4

Accession For
NTIS GRA&I [X]
DTIC TAB [ ]
Unannounced [ ]
Justification
By
Distribution/
Availability Codes
Dist | Avail and/or Special
A-1

classification

title	: unclassified
abstract	: unclassified
report	: unclassified

no. of copies	: 27
no. of pages	: 45
appendices	: --

date : november 1989

All information which is classified according to Dutch regulations shall be treated by the recipient in the same way as classified information of corresponding value in his own country. No part of this information will be disclosed to any party

DISTRIBUTION STATEMENT A
Approved for public release;
Distribution Unlimited

DTIC ELECTE AUG 07 1990 S D E

TNO

report no. : FEL-89-B336
title : Measurement results of the FEL-TNO planar rectangular near field facility (1978-1989)

author(s) : Ir. J.G. van Hezewijk
institute : TNO Physics and Electronics Laboratory

date : November 1989
NDRO no. : n.a.
no. in pow '89 : 710,2

ABSTRACT

This report describes the most important results of measurements, which have been performed with the rectangular planar near-field facility of the FEL-TNO laboratory from 1978 to 1989.
Various types of antennas have been measured in this period.
The radiation (both sum and difference) patterns of antennas with narrow main beams can be determined with great accuracy.
This is true as well for antennas, which have dimensions, that are equal or slightly larger than the measurement frame of the near field scanner, or that have a broad main beam in one plane.
Besides, the near field measurement facility offers the possibility to detect defective radiating elements in a large array antenna very fast.
If a parameter, like the frequency or the scan-direction of the main beam, can be changed very quickly, then we can determine more radiation patterns of an antenna during the time needed to perform one single near field measurement.
The reported measurements give a good overview of the possibilities of the planar near field measurement technique.

rapport no. : FEL-89-B336
titel : Meetresultaten van de rechthoekige planaire nabije-veld meetfaciliteit van het FEL-TNO (1978-1989)

auteur(s) : Ir. J.G. van Hezewijk
instituut : Fysisch en Elektronisch Laboratorium TNO

datum : november 1989
hdo-opdr.no. : n.v.t.
no. in iwp '89 : 710,2

SAMENVATTING

Dit rapport beschrijft de belangrijkste resultaten van metingen, die zijn uitgevoerd op de rechthoekige planaire nabije-veld meetfaciliteit van het FEL-TNO van 1978 tot 1989.
Diverse typen antennes zijn in deze periode onderzocht.
Deze planaire meetbaan blijkt bijzonder geschikt te zijn voor het bepalen van de stralingsdiagrammen (som- en verschilpatronen) van antennes met een smalle hoofdbundel.
Dit geldt tevens voor antennes, waarvan de afmetingen in de orde van grootte van het beschikbare meetvlak liggen, en voor antennes, die in een vlak een brede hoofdbundel hebben.
Daarnaast biedt de planaire meetfaciliteit de mogelijkheid om snel defecte elementen op te sporen van een array antenne, die uit vele honderden elementen bestaat.
Indien een parameter, als de frequentie of de scan-richting van de hoofdbundel, van een antenne snel veranderd kan worden, kunnen er verschillende stralingsdiagrammen bepaald worden gedurende de meettijd van een enkele nabije veld meting. Dit rapport beoogt een duidelijke indruk te geven van de mogelijkheden van nabije-veld metingen.

1 INTRODUCTION

This report contains some significant results of measurements, which have been performed at the planar near field facility of the Physics and Electronics Laboratory of TNO (FEL).
This planar near field facility was put into operation in 1978 and was the first of its kind in the Netherlands. Many measurements at C-band frequencies have shown that the planar near field measurement technique can be applied successfully for various types of antennas. The calculated radiation patterns from data obtained with near field measurements, agree very well with radiation patterns measured on the FEL-TNO far field test range.
Now, 11 years later, the planar near field facility is being revised. Stepping motors have been replaced by servo motors and some local intelligence has been installed, which controls these motors. The old system could only measure at three frequencies at C-band. We will now be able to perform measurements at frequencies up to 18 GHz.
This revision offers us a good moment to summarize the measurements, which have been performed so far.
This report reviews only the most significant measurements. The measurement results of 4 different types of antennas will be discussed:

- A (pencil beam) front fed parabolic antenna (§ 3.1)
  Given here are the different types of plot, that can be made (§ 3.1.2 and § 3.1.3) and the verification of the calculated far field pattern with the far field patterns as measured at the FEL-TNO far field antenna test range.

- A slotted waveguide planar array (§ 3.2)
  This is a large rectangular antenna. One of the sides of its aperture is nearly equal to the size of the square measurement plane. A substantial portion of the electric field of this antenna radiates outside the measurement plane and therefore the calculated radiation pattern will be less accurate. The technique of combining two near field data sets to get the far field radiation pattern of this very large antenna, is successfully performed (§ 3.2.2).
- A beam shaped cosecans-squared antenna (§ 3.3)
  Though this antenna has a radiation pattern, that is very broad in one plane, we can measure it correctly with a near field facility. We are able to get the radiation patterns for different frequencies within one near field measurement. This is called "multiplexing" (§ 3.3.2). It will be illustrated for this antenna.
- A planar phased array antenna : CAISSA (§ 3.4)
  This antenna consists of more than 800 radiating elements. Each element has its own phase shifter. We'll illustrate in section 3.4.3, that defective phase shifters can be detected very fast with the results from one near field measurement. Difference patterns can be calculated with confidence (§ 3.4.4).

This discussion is preceded by a description of the planar near field facility at FEL-TNO.(1978-1989)
The conclusions of this report are listed in chapter 4.
The planar near field measurement theory will not be found in this report. It has been described many times in literature[3,4]. The reader is expected to be familiar with this theory.

2. THE FEL-TNO PLANAR NEAR FIELD FACILITY

The planar near field facility has been built up in 1978.
It consists of a 3*3 meter^2 scanner, which is restricted to an usable area of 2.5*2.5 meter^2, because of applied absorbing material as shown in Figure 1.1.
A photograph of this facility is given in Fig 1.1, in which an antenna under test (AUT) is installed:

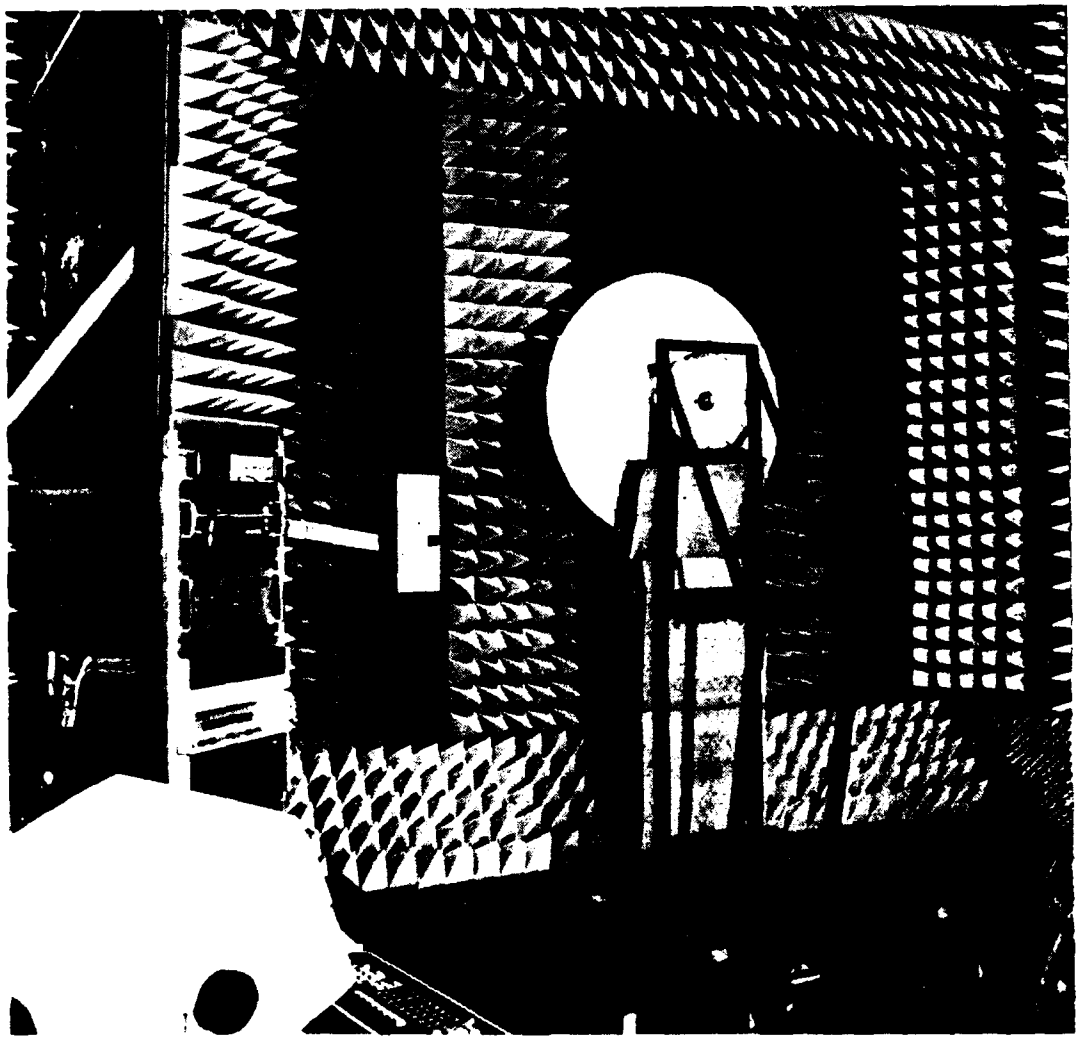

Fig 1.1 Planar near field facility at FEL-TNO

The block-diagram of the facility is shown in Fig 1.2:

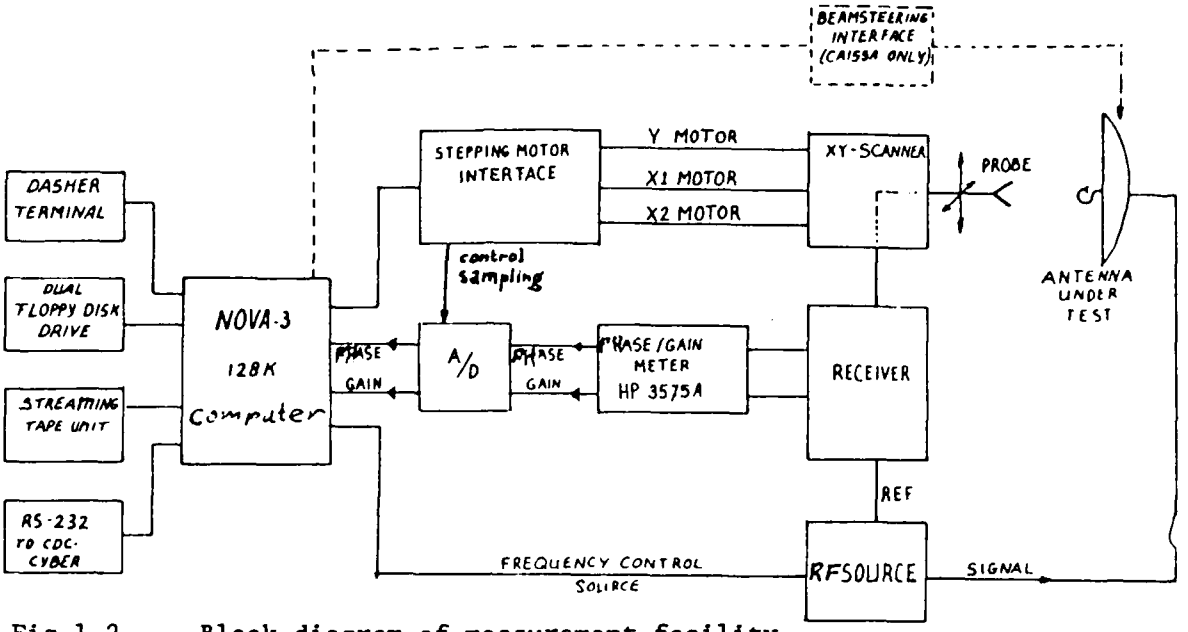

Fig 1.2 Block diagram of measurement facility

Measurement procedure

The measurement procedure is as follows:
The electric field of a transmitting AUT is measured in a rectangular grid on the measurement plane. The distance between the samples in horizontal and vertical direction is about 1/3 to 1/2 wavelength.
The probe is moved over the measurement surface under computer control. When the probe is at a measurement point (determined by the computer, which calculates the desired number of steps to be made by the motors) then the electric field will be measured and stored.

Components of the FEL-TNO near field facility

The block diagram shows the way the measurement procedure is executed at the FEL-TNO facility. The amplitude and the phase of the electric field are continuously measured by the receiver and is given (analog) to the phase-gain meter, that displays the measured amplitude and phase and transfers it in a correct form to the Analog/Digital Converter. If the computer notices that a sample point has been reached, then it gives a signal to the stepping motor interface. This interface gives a control

sampling signal to the A/D-converter and the digital data will be stored in the computer.
It takes the computer a lot of time to control the stepping motors and check whether a sample-point has been reached. It proved to be impossible to make near field measurements with sample spacing less than about 1.7 cm. Thus, near field measurements at higher frequencies could not be executed. The stepping motors are in the new near field facility (in operation from 1989) replaced by servo motors with local intelligence, that controls the servo motors and determines whether a measurement point has been reached.
The first receiver and source have been built at the FEL-TNO laboratory. Later on, a Scientific Atlanta receiver (SA1782) has replaced the receiver and a HP sweeper has replaced the source. This HP-sweeper is phase-locked by an EIP frequency counter. The frequency stability is better than 10^{-7}.
The beamsteering interface in Fig. 1.2 is only used when the CAISSA phased array antenna (§ 3.4) is measured. It enables the CAISSA antenna to change its scan direction within microseconds for multiplexed measurements (§ 3.4.4).
If a measurement is completed, then the data is stored on tape or send to the central computer system (CYBER).

Calculations

The measured near field data serves as input for a software program (based on the package of National Bureau of Standards) that calculates the uncorrected radiation pattern of the antenna under test. This is also called the "wavenumber spectrum". The calculations consist mainly of a two-dimensional Fourier transformation, which is performed at the central computer and can be calculated very fast if the number of samples in each direction is of a power of 2.
This wavenumber spectrum has to be corrected for the sensitivity of the probe used for both electromagnetic waves from different direction as well as the polarisation. This probe-correction leads to the desired (probe-corrected) far field radiation pattern of the AUT.

This probe-correction for the co-polarised component of a linearly polarized TEM wave corresponds to a multiplication of the uncorrected radiation pattern with the factor $\cos(\theta)/E_p(\theta,\varphi)$, where $E_p(\theta,\varphi)$ is the probe far field pattern in the direction (θ,φ) [2, p.13], when the cross-/co-polarisation ratio of the probe is very small.
A Geyerhorn with 2 grooves satisfies this condition. Further it has the advantage of an approximately circular symmetric amplitude pattern (no φ-dependency) and an approximately constant phase for angles $|\theta| < 70°$. The probe-correction is then a simple scalar multiplication. Therefore this Geyerhorn is chosen as probe for the near field measurements.
The difference between uncorrected and probe corrected radiation patterns is then that the level of the sidelobes for angles far off axis ($|\theta| < 60°$) of the uncorrected radiation pattern will be lower.

Data representation

Graphical representations of near- and far field data in the form of 2-, 3-dimensional and contour plots are obtained on the central computer facilities of the laboratory. Examples can be found in § 3.1.2 and § 3.1.3.

Other details

The probe moves column wise over the plane during a measurement, starting in the upper left corner. The odd columns are measured with the probe moving downward, the even ones in an upward direction. This is called a "bi-directional" or "alternating" probe movement. The measurements with bi-directional probe movement are twice as fast as measurements with a uni-directional probe movement. It takes two hours to perform a near field measurement. The probe speed is 40 mm/sec.
The dynamic range of the FEL-TNO planar near field facility is better than 50 dB.
Mentioning more details about the set-up of this facility would be beyond the scope of this report. Besides, the new facility set-up differs in many aspects from the set-up shown here, as can be read in a report, that will be published in the near future.

3. RESULTS OF MEASUREMENTS

3.1 Front Fed Parabolic Antenna

3.1.1 Description of the antenna

A (pencil beam) front fed parabolic antenna with a diameter of 1.1 meters (about 20 wavelengths at C-band) has been used in these measurements.

Figure 3.1.1 shows this antenna configuration:

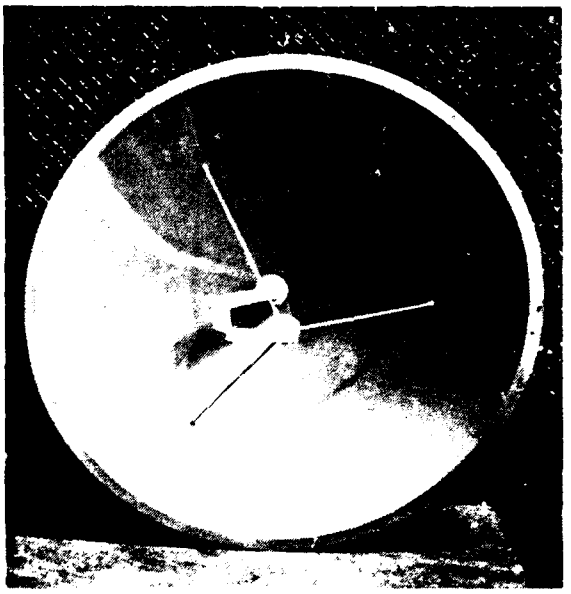

Fig 3.1.1 The front fed parabolic antenna

The horn in the focal point of the reflector is fed via a waveguide-run in the H-plane and radiates a linearly polarised wave. This horn is supported by 3 struts.

The distance between the aperture of the AUT and the probe (d) determines the maximum angle θ_{max} , for which reliable far field patterns can be calculated with near field data, according to the following relation:

$$\theta_{max}=\arctan((L-a)/2d) \qquad (3.1.1)$$

with L= length of measurement plane

a= aperture diameter

The distance "d" is often about 2 or 3 wavelengths. The feed in the focal point of a reflector often restricts the possibility to choose d so small.

With L=2.50 m, a=1.10 m and d=0.38 m, $\theta_{max}\approx 60°$.

3.1.2 Near Field Data

The near field data (amplitude and phase) can be graphically represented in 2D-,3D- or contour plots.

Examples of a 3D-plot of the measured near field amplitude and contour plots of the measured near field amplitude and phase are given in Fig 3.1.2/3/4:

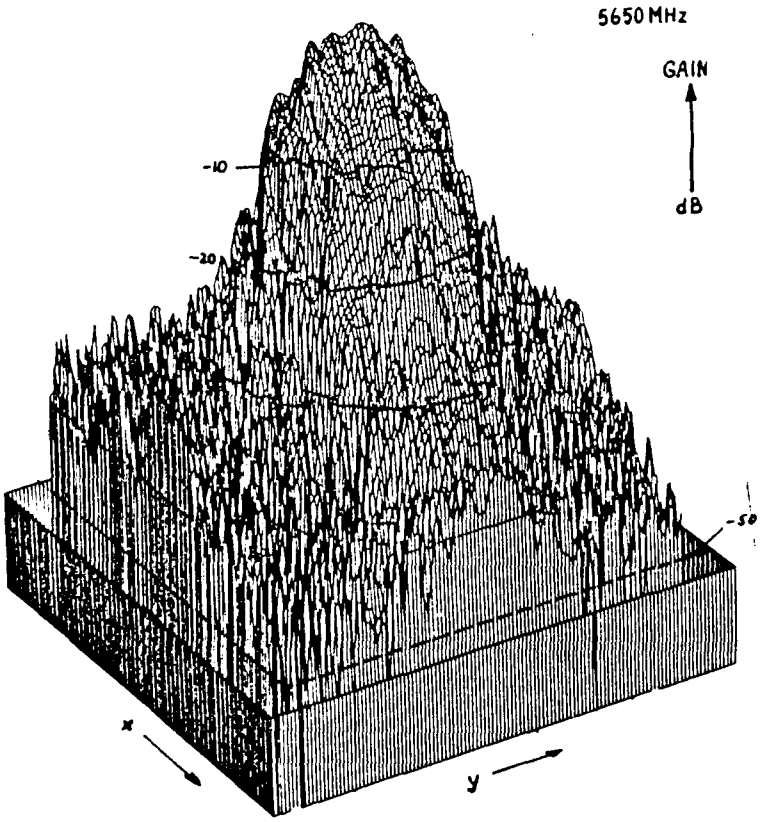

Fig 3.1.2 3D-plot of measured near field amplitude (freq=5650 MHz) (data is normalized)

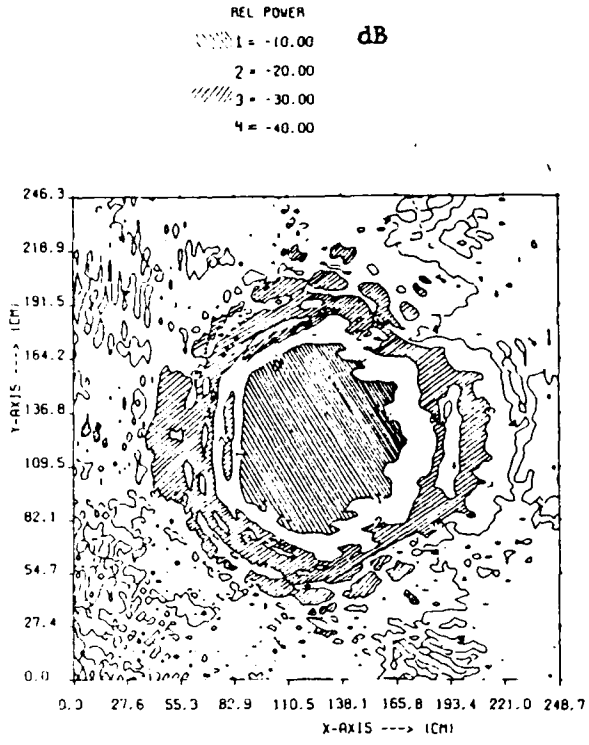

Fig 3.1.3 Contour plot of measured near field amplitude(freq=5650 MHz)

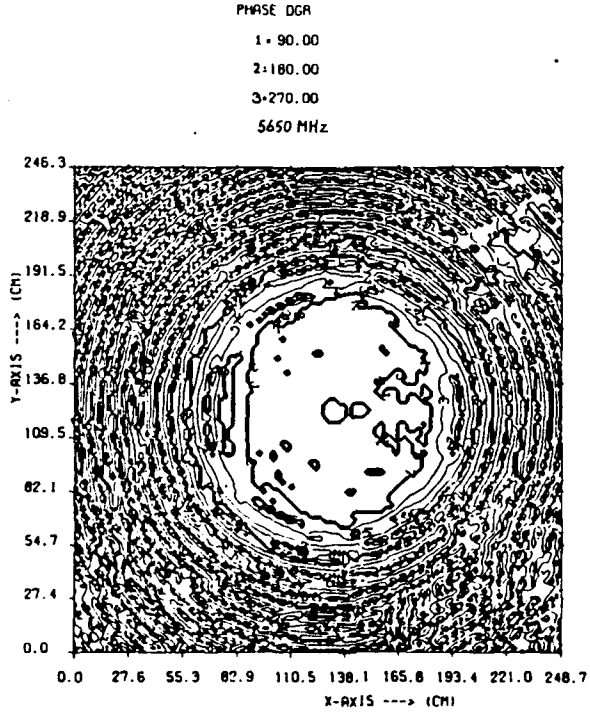

Fig 3.1.4 Contour plot of measured near field phase (freq=5650 MHz)

The near field contour plots show clearly that the aperture field is not so nice and less circular symmetric as one might expect. This is caused by the blocking and diffraction caused by the feed and the struts.
The amplitude of the electric field at the edge of the measurement plane is -40 dB or less.

3.1.3 Calculated Versus Measured Far Field Radiation Patterns

The uncorrected radiation pattern(or "wavenumber spectrum" from page 11) is given in Fig 3.1.5:

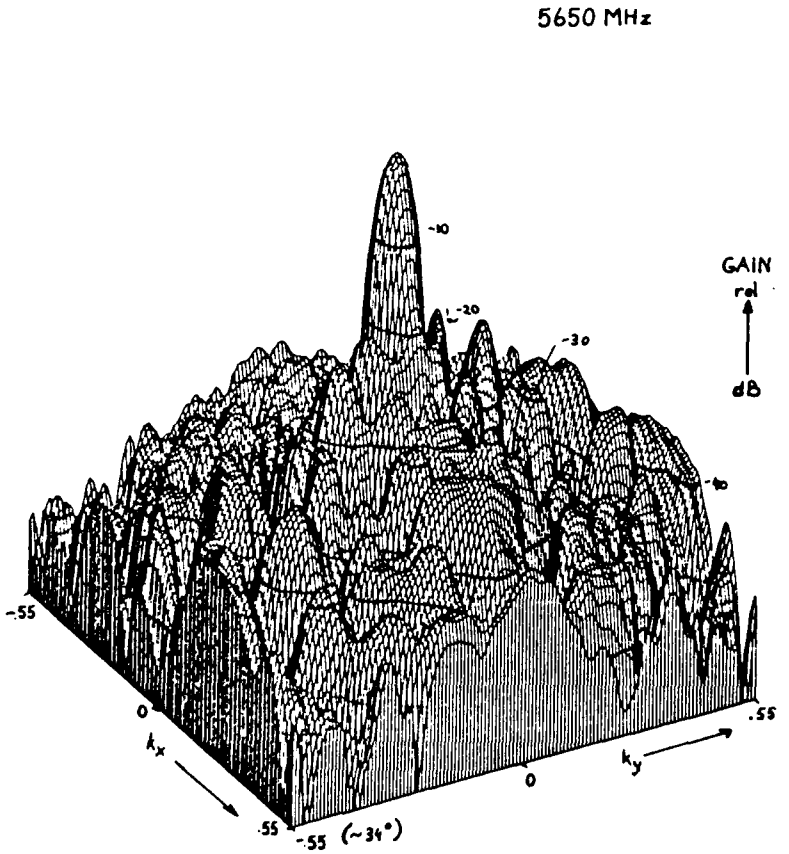

Fig 3.1.5 Uncorrected radiation pattern of front fed parabolic antenna (freq=5650 MHz)

In the following of the report, we'll mostly show probe-corrected radiation patterns, which will be called "*calculated radiation patterns*", instead of not-corrected radiation patterns. "*Measured radiation patterns*" are radiation patterns obtained from far field measurements.

Probe corrected amplitude patterns are compared in Figure 3.1.6 with measured far field patterns:

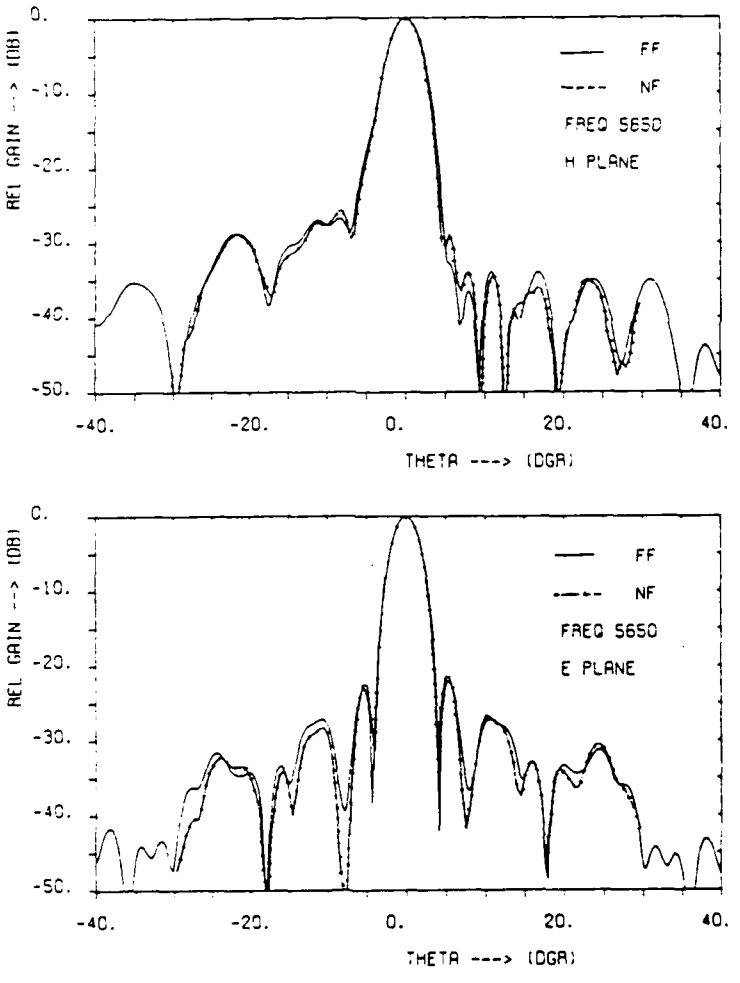

NF=Near Field FF= Far Field

Fig 3.1.6 Comparison between calculated and measured far field amplitude patterns in the E- and H-plane of the parabolic front fed antenna($\theta < \pm 30°$, freq=5650 MHz)

Due to a two-dimensional filtering technique to obtain high angular resolution [5, p.28], the calculated far field patterns are limited to angles $|\theta| < 30°$.

The radiation patterns agree quite well.

The maximum deviations are about 1 to 2 dB at -30 dB below the maximum of the beam. But the behaviour of the patterns agrees also quite well for lower levels.

The filter technique can't be applied to obtain high angular resolution for large angles θ.

The radiation patterns for larger angles θ are shown in Figure 3.1.7:

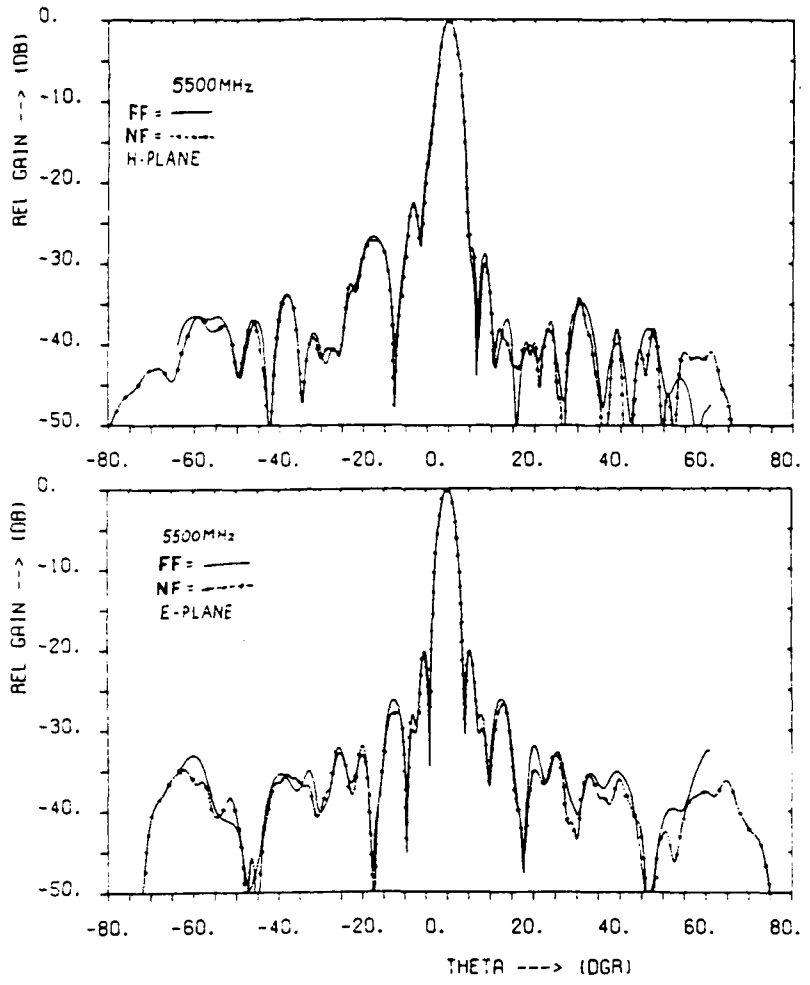

Fig 3.1.7 Comparison between calculated and measured far field amplitude patterns of the front fed parabolic antenna in the E- and H-plane ($\theta < \pm 60°$, freq=5500 MHz)

These measurements show clearly that the with equation (3.1.1) deduced $\theta_{max} \approx 60°$ is correct. Larger differences between the calculated and the measured far field patterns occur at lower levels and for larger angles. We must, however, keep in mind that at lower levels the far field range also introduces some errors. A typical error at a -30 dB level for a good far field test range is 1 dB.

Conclusion

We may conclude this section by stating that the radiation patterns of pencil beam parabolic front fed antennas can be determined with great accuracy with a near field facility. The differences between the calculated and measured far field pattern clearly become larger at lower levels and larger angles θ.

3.2 Slotted Waveguide Array

3.2.1 Description of the antenna

The measured planar array antenna consists of 20 waveguides with non-resonant slots [1, p.595]. The main beam radiates in a direction off broadside, that is dependant on frequency. The waveguides are fed on one side and characteristically terminated with a load at the other side. The distribution of the available power is performed by a sort of "space fed" construction. An E-plane horn with a polystyren lens distributes the power. The slotted waveguide array is designed for a sidelobe level less than -36 dB.

The measured slotted waveguide array, is shown in Fig 3.2, where it is placed in the near field facility:

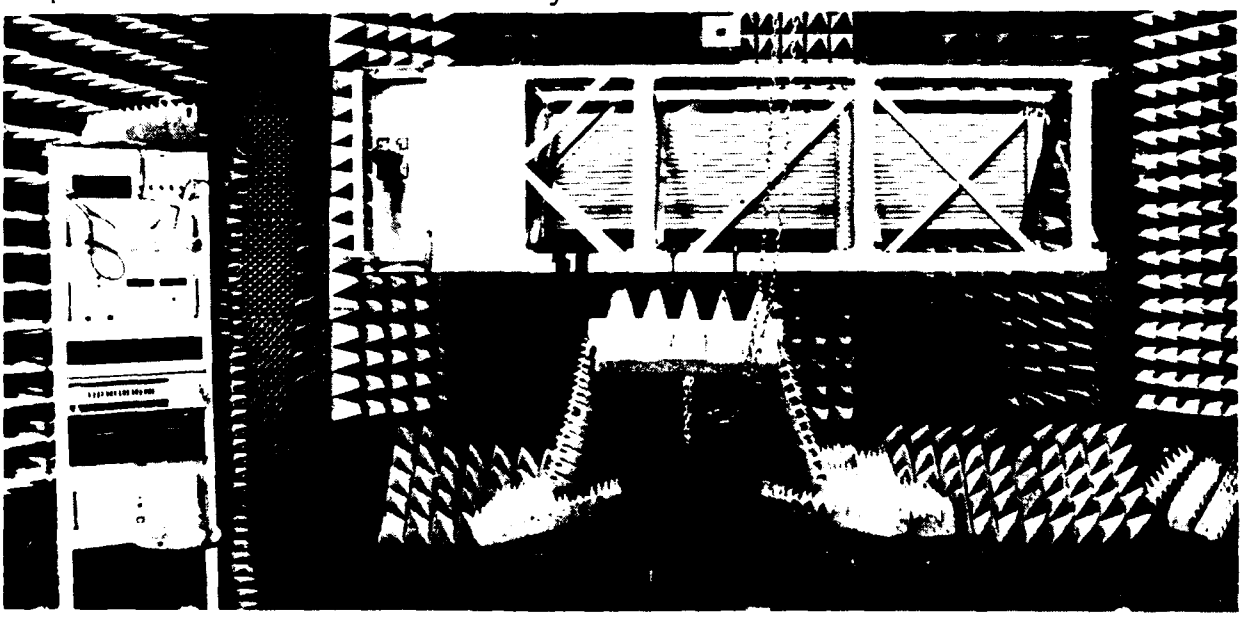

Fig 3.2.1 Slotted waveguide array in near field facility

The aperture of the slotted waveguide array is 2.4 meters in horizontal direction. Only 10 cm smaller than the usable measurement plane !
The planar array can be moved in horizontal direction along the measurement plane parallel to the scanner.

3.2.2 Combination Of Near Field Data Sets To Get One Far Field Radiation Pattern

It will be dificult to calculate the radiation pattern of an antenna (like this one) with a great accuracy, if a substantial portion of the electric field radiates outside the measurement plane.

We'll see in this section that we can measure in the FEL-TNO near field facility antennas with aperture dimensions, which are comparable or slightly larger than the measurement plane: we extract a final near field data set from more than one measurement. This final data set is used as input for far field calculations.

In our situation, we have performed 2 measurements over the whole measurement plane. In the second measurement, the array was displaced exactly 28 sample-spacings in the horizontal direction parallel to the scanner. Each measurement was performed over 100 columns and 128 rows. We then get 2 data sets consisting of 100 columns, where the first 72 columns of the first data set should be exactly the same as the last columns of the second data set. This overlap-part can be used to put the data sets together to 1 final data set, consisting of 128x128 datapoints. See Fig 3.2.2.

Figure 3.2.2 shows the measured amplitude and phase of the 2 data sets:

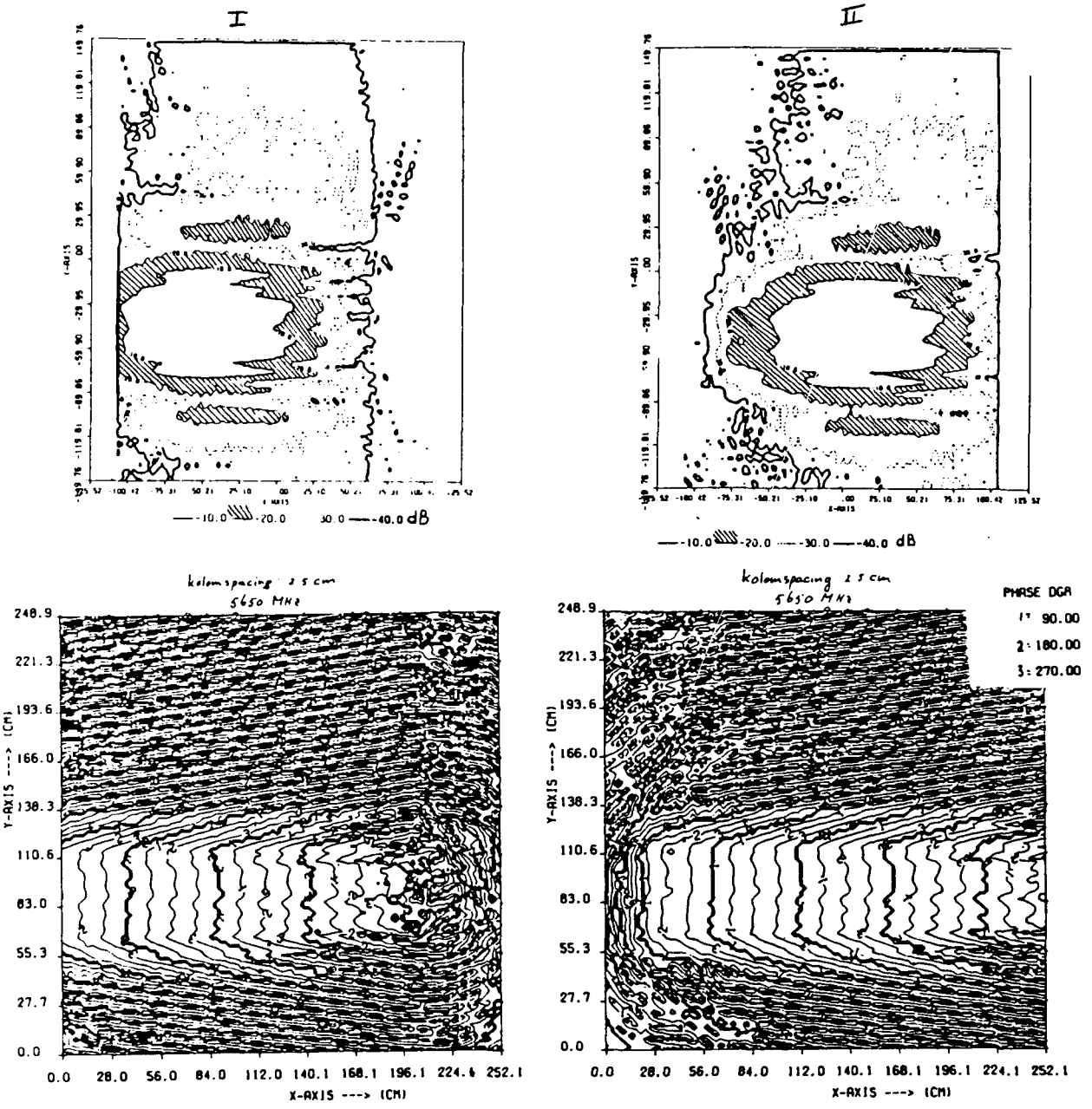

Fig 3.2.2 Contour plots of the amplitude and phase of two data sets, as measured with a small displacement of the slotted waveguide antenna in the horizontal direction

The measured phase in the data sets is used to perform this combination. We can see clearly the overlap of the 72 columns in the amplitude contour plots. The overlap is less obvious in the phase plots due to the phase gradient over the aperture of the antenna.
A small extra phase (± 20°) had to be added to one data set in order to get the final data set.
It must be emphasized that the displacement of an AUT has to be performed very accurately.
Suppose that the distance 'd' between the AUT and the probe changes during a displacement, then a constant phase difference between will exist between the overlapping points of the 2 measurements. The amplitude can differ as well.
If the displacement is not an exact whole number of sample-spacings, then there are no points in the second measurement that overlap points of the first measurement.
If the aperture distribution of the AUT has a linear phase-gradient, then a constant phase difference will exist between these "semi" overlapping points of the two measurements. The influence of such a displacement error is less for an AUT with its main beam in broadside-direction.
Rotation errors in θ-direction of the AUT due to the displacement will lead to a squint of the main beam. This error can be corrected with a linear phase shift over the near field data.
The elegance of the method disappears, however, if many corrections have to be applied.
This antenna needed an additional phase shift of 20° probably due to a small displacement error in horizontal direction parallel to the scanner. Rotation errors seem to be absent.
The virtual enlargement of the measurement plane is equal to the displacement. In this case 28 sample spacings.(≈ 70 cm)
This enlargement is very important. It increases the range of angle θ, for which far field patterns can be determined with near field data.

An example: if we use Eq. (3.1.1) and we assume that the distance between the apertures of the probe and the AUT is 5 wavelengths, then we find the maximal angle θ_{max}, for which reliable far field patterns can be calculated with near field data, increases from 11° to 56°!
The calculated radiation patterns of both data sets are plotted in Fig 3.2.3:

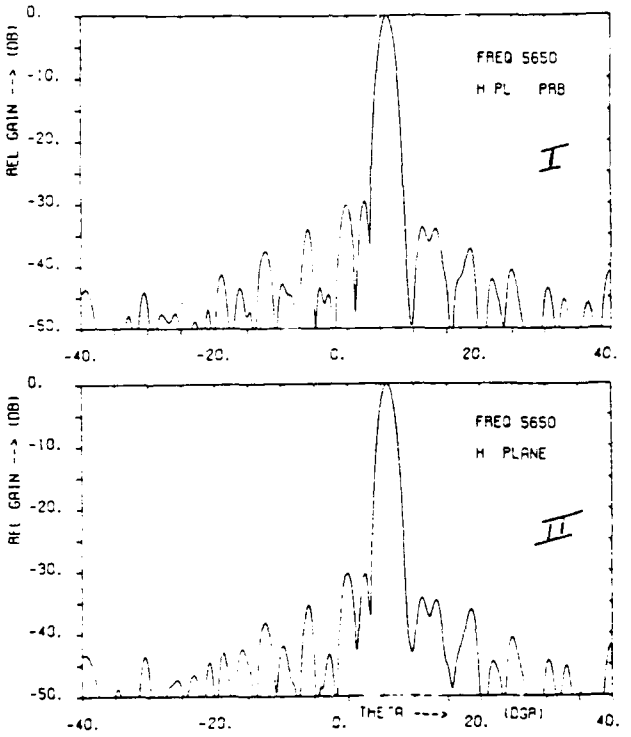

Fig 3.2.3 Calculated H-plane radiation pattern of slotted waveguide array for first and second data set of Figure 3.2.2

The radiation patterns differ.

The uncorrected H-plane radiation pattern calculated from the final data set is shown in Fig 3.2.4:

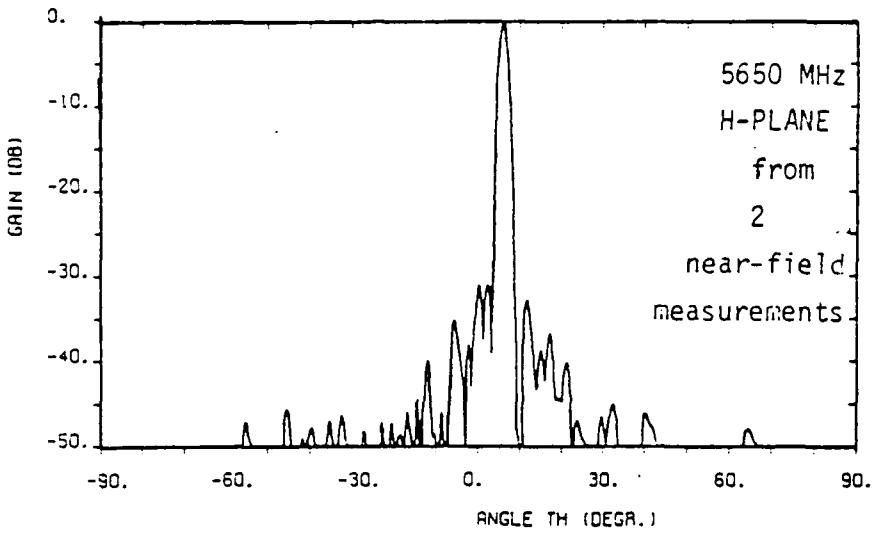

Fig 3.2.4 Uncorrected H-plane radiation pattern of slotted waveguide array obtained with the final near field data set (freq=5650 MHz)

The uncorrected radiation pattern, as calculated with the final data set differs from the probe corrected radiation patterns calculated with one single data set. Especially for the first sidelobes.
The calculated radiation pattern of the final data set might be compared with measured far field radiation patterns. The last measurements are, however, not available and this interesting comparison can not be made.

Conclusion

We may conclude at the end of this section, that it is possible to measure antennas in a near field facility with aperture dimensions equal or larger than the measurement plane.
More than one measurement should be made with the AUT translated in the direction in which its aperture dimension is largest.
This displacement has to be done very accurately!
The measured phase has to be used to combine the measurement to one final data set, from which the radiation pattern can be calculated.

3.3 Shaped Beam Cosecans-Squared Antenna

3.3.1 Description of the antenna

The shaped beam cosecans-squared antenna is shown in Figure 3.3.1:

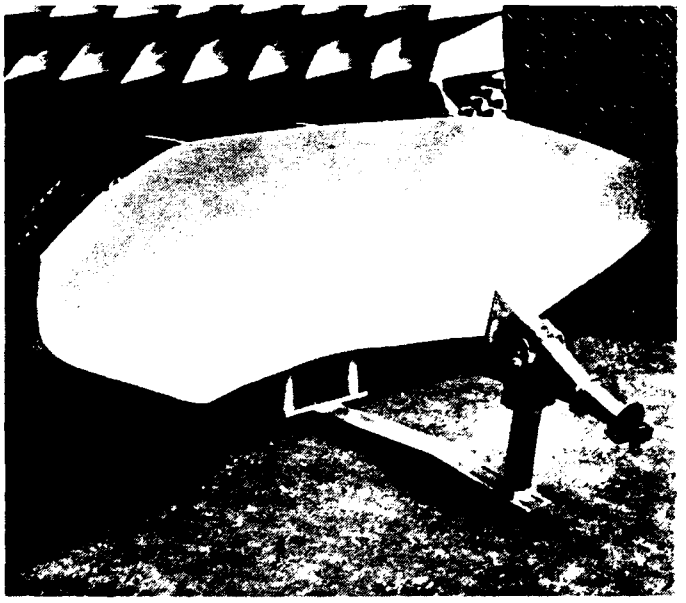

Fig 3.3.1 The shaped-beam cosecans-squared antenna

As stated before, it is difficult to compute the far field pattern of an AUT from planar near field measurements with great accuracy, if a substantial portion of the electric field of the AUT radiates outside the measurement plane.

In this section we have such an antenna: the shaped beam cosecans-squared antenna.

This antenna produces a beam with a small beamwidth in the azimuth- and a very large beamwidth in the elevation direction. The shape of the beam in elevation direction should agree to $f(\theta_e)$=cosecans$^2(\theta_e)$, where θ_e is the elevation angle. The situation as described above might occur. Not very accurate calculated radiation patterns can result.

The distance 'd' should be small, especially for broad beam antennas, in order to pick up as much electric field of the AUT in the measurement plane as possible.

The feed in the antenna (Fig 3.3.1), however, restricts the choice of a small distance 'd' between the aperture of the antenna and the measurement plane.
We'll compare in the following section the calculated and measured far field radiation patterns. We'll also investigate the influence of multiplexing on the calculated radiation patterns.

3.3.2 Calculated Versus Measured Far Field Radiation Patterns

Figure 3.3.2 shows the calculated and measured far field radiation patterns of the cosecans-squared antenna:

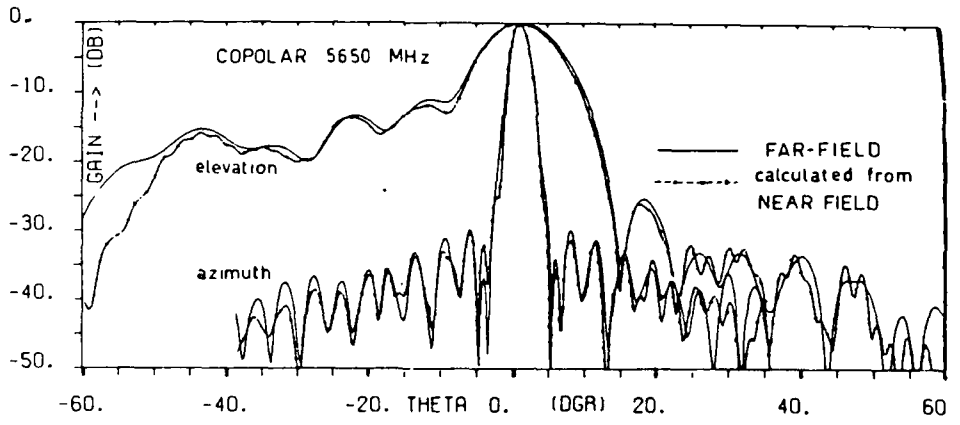

Fig 3.3.2 Calculated and measured radiation patterns of the cosecans -squared antenna in elevation and azimuth plane

The agreement is very good in the azimuth and elevation plane. The differences in the elevation plane become larger for θ<-40°. This can be explained by the fact that too much electric field of the AUT is radiated outside the measurement plane.

3.3.3 Multiplexing

The probe moves with a constant velocity over the measurement plane and does not stop at each measurement point. If we perform more than one

measurement between two samples, then we can perform more measurements during the time of one near field measurement. This is called "multiplexing". Parameters like the frequency or scan-direction of the AUT might be changed for instance. (See the beam-steering interface for the CAISSA antenna in Fig 1.2)

Because each near field measurement takes about 2 hours, multiplexing is an attractive feature to reduce the overall testing time, when more than one pattern has to be measured of an antenna.

It has to be proved first, however, that multiplexed and not-multiplexed near field measurements lead to identical far field patterns, if the Nyquist criterium is met.

A test, which shows whether multiplexing may be applied for a certain AUT can be as follows: Perform multiplexing, but do in this case not change any parameter of the AUT ,like the frequency or the scan direction. We should obtain nearly identical radiation patterns.

Or one might compare the radiation patterns of an AUT, obtained from a near field measurement with and without multiplexing.

This last mentioned test is performed for the cosecans-squared antenna. The measurement plane of the near field measurement with multiplexing was shorter than for the near field measurement without multiplexing.

Fig 3.3.3. shows the results of these tests:

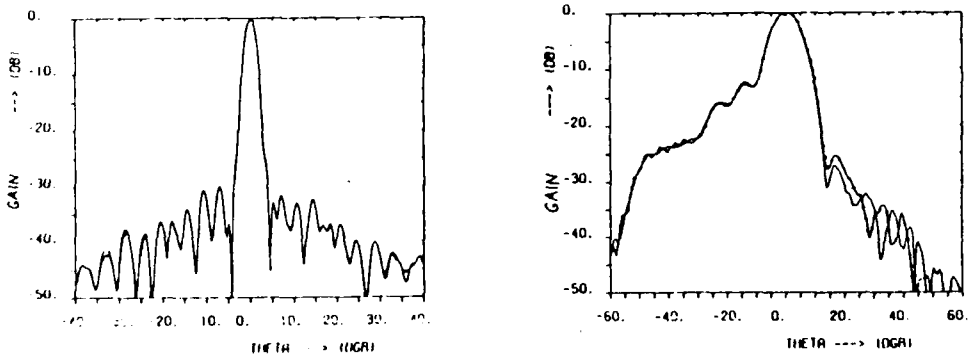

azimuth plane elevation plane

Fig 3.3.3 Radiation patterns of the cosecans-squared antenna in the elevation and azimuth plane obtained from near field measurements with and without multiplexing

The differences in radiation patterns in the elevation plane are too large. The smaller measurement plane, as used in the measurement with multiplexing, explains differences for large angles θ, but the difference of 1.5 to 2 dB for the first sidelobe can't be concluded. The radiation patterns for the "negative" angles θ agree much better.
The radiation patterns in the azimuth plane are nearly equal. It can be concluded from Fig 3.3.3 that multiplexing is admitted for pencil-beam antennas.

Conclusion

Antennas with a small beam in one plane and a broad beam in the other plane, like the cosecans squared antenna, can be calculated with high accuracy in the near field facility.
Multiplexing can be applied for pencil-beam antennas to reduce the near field measurement time.

3.4 Planar Phased Array Antenna (CAISSA)

3.4.1 Description of the antenna

The CAISSA antenna is a planar, space-fed, phased array antenna, that has been designed and constructed at FEL-TNO.
It consists of 849 radiating elements and 325 dummy elements, of which the last are placed at the circumference of the antenna.
The radiating elements of the array are open-ended waveguides of rectangular cross-section. The radiating elements are arranged in a doubly periodic grid.
The radius of the planar array is 42.5 cm.
Figure 3.4.1 shows the functional block diagram of the transmitting CAISSA antenna [6]:

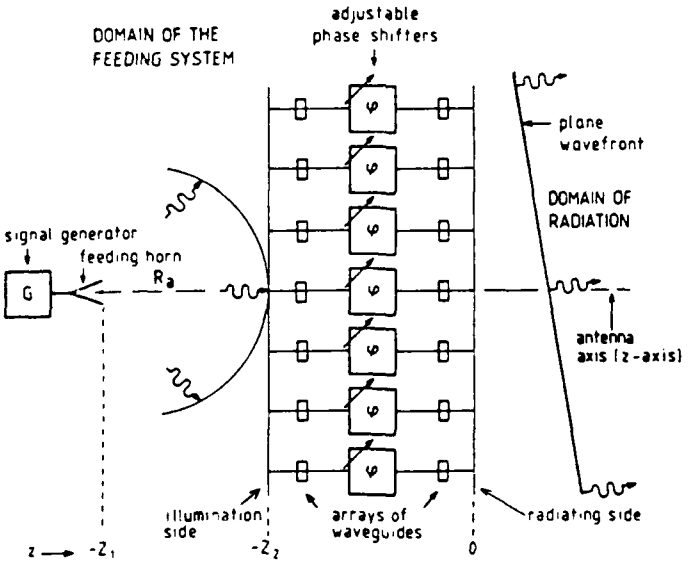

Fig 3.4.1 Functional block diagram of the transmitting CAISSA antenna

In the transmitting mode, the antenna is illuminated by a coherent incident field originating from a feeding horn, whose axis coincides with the axis of the antenna. At the illumination side of the antenna, the incident wave is partially reflected and partially transmitted. The transmitted wave passes through a first array of waveguides, next

through an array of adjustable phase shifters and then through a second array of waveguides.

The phase shifters have a two-fold purpose, viz:

1) they perform the phase correction that transforms the primary wave from the feeding horn into one with a plane equi-phase surface, parallel to the plane of the antenna,

2) they accomplish a certain additional phase shift between two adjacent elements in order to steer the radiated beam in a prescribed direction.

In order to reduce edge effects at the rim of the antenna, so-called dummy elements have been attached. These dummy elements are installed in order to ensure that all radiating elements have an equal environment. Each phase shifter is controlled digitally and is adjustable with an accuracy, that is determined by the number of available bits(=4 bits). The CAISSA antenna can operate in a sum and a difference mode.
The following figure shows the CAISSA antenna mounted in the FEL-TNO near field facility:

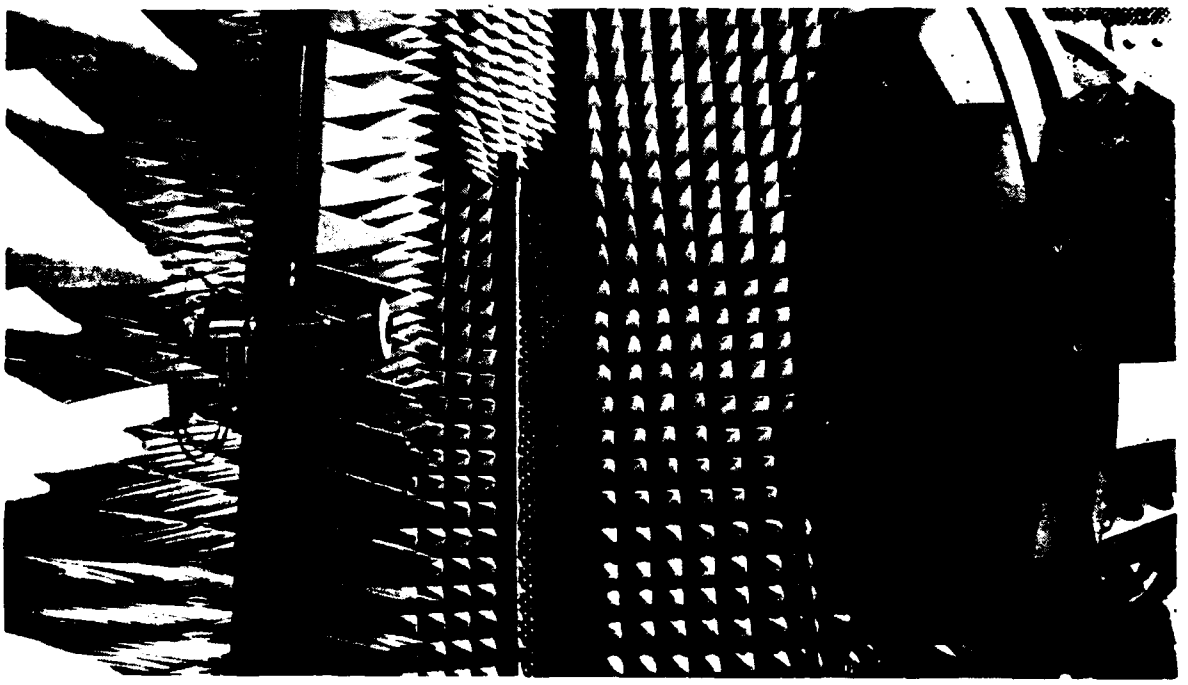

Fig 3.4.2 CAISSA antenna mounted in the FEL-TNO near field facility

3.4.2 Patterns For Different Scan Angles

The phase-shifters are adjusted such that the main beam of the far field points to the directions θ=0°, 45° and 60° in the H-plane.

Fig 3.4.3 shows contour plots of the measured near field amplitude and phase for these three different scan angles at a frequency of 5500 MHz:

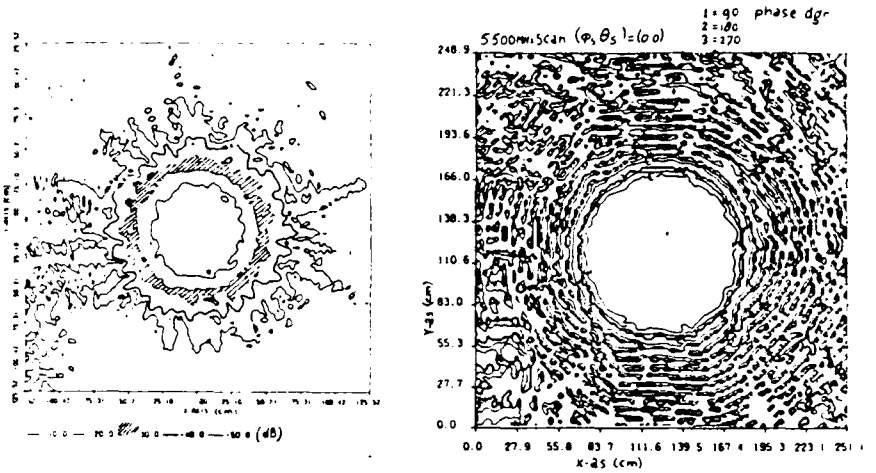

$\theta_S = 0^0$

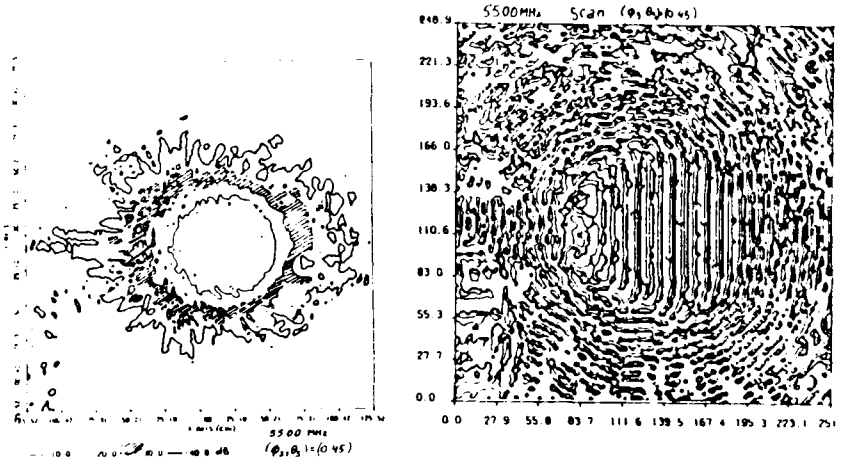

$\theta_S = 45^0$

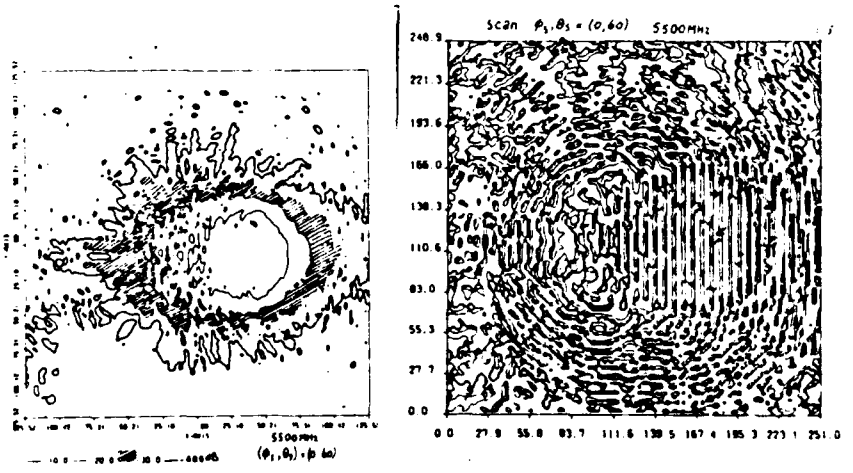

$\theta_S = 60^0$

Fig 3.4.3 Contour plot of measured near field amplitude and phase for scan angles θ=0°,45° and 60° in the H-plane. (Sum pattern, Freq=5500 MHz)

The linear phase-shift that we expect for scan angles $\theta \neq 0$ is clearly present.

The far field antenna patterns, calculated with this data, are shown in Fig 3.4.4:

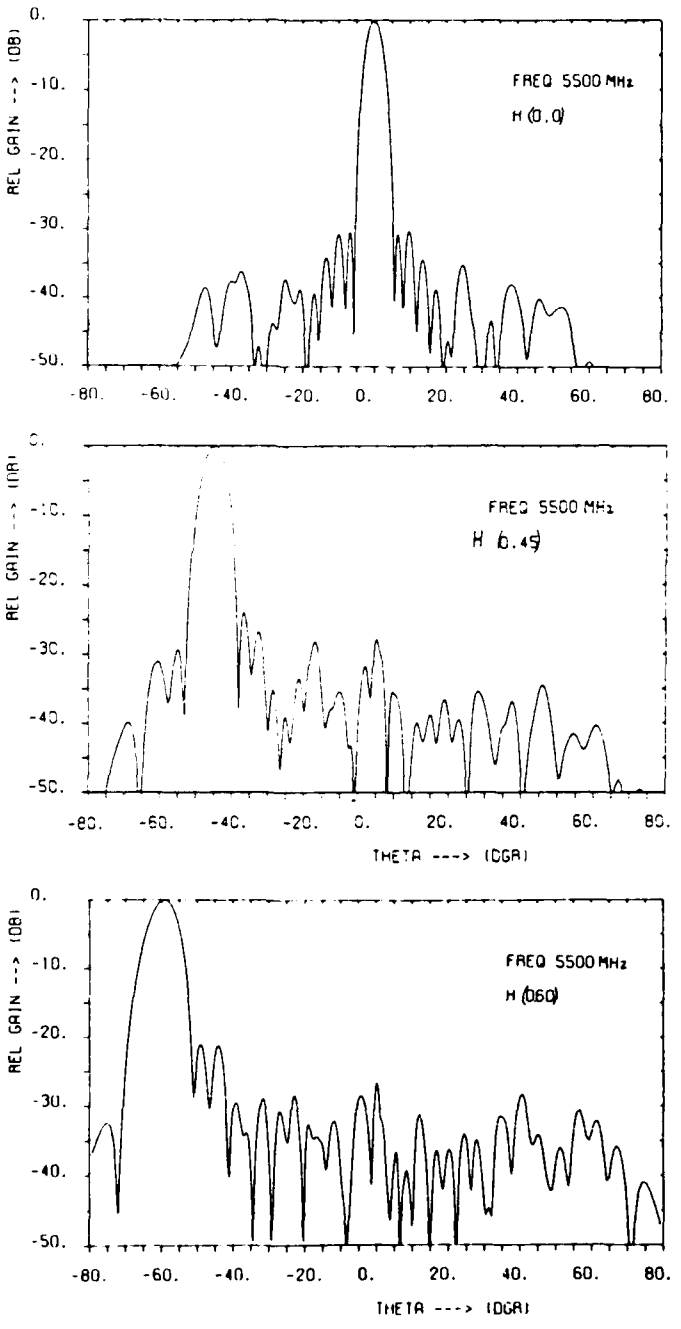

Fig 3.4.4 Calculated far field amplitude pattern for scanangles θ=0°, 45° and θ=60° in the H-plane.Sum pattern, Freq=5500MHz

The patterns are normalized. On first hand might be concluded from this figure that the sidelobes of patterns with larger scan angles become larger. This is true, but it is partly caused by the gain-degradation of the main beam as a function of the scan angle.
The comparison between the calculated and measured far field patterns is made for the CAISSA antenna with main beam at broadside at a frequency of 5500 MHz (See Figure 3.4.5 for the measured radiation pattern)

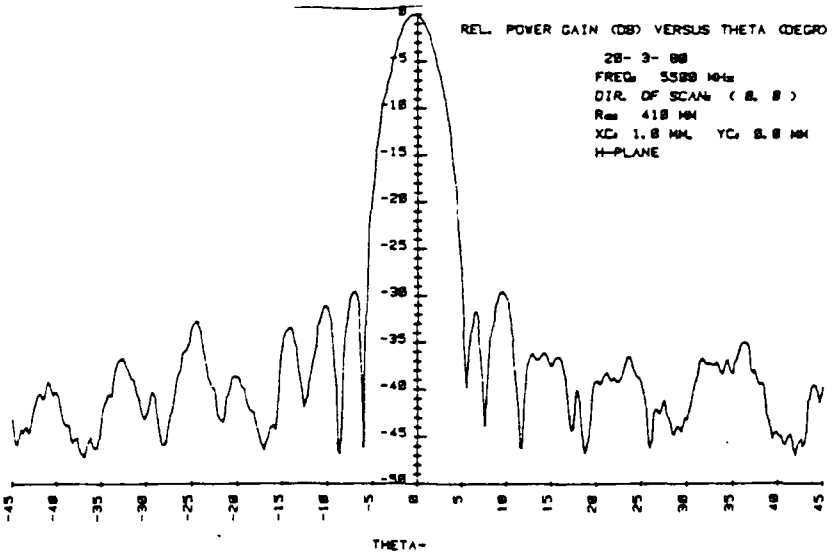

Fig 3.4.5 Measured radiation pattern of the CAISSA antenna with the main beam at broadside (Freq= 5500 MHz)

The calculated pattern can be seen in Fig 3.4.4.
We must remark, that the measured pattern is made 2.5 years before the near field measurements took place and that several repairs have been performed on the CAISSA antenna in this period.
The receiver used in 1980 for these far field measurements did not have the required dynamic range, so that errors occur below the -35 to -40 dB level.
The patterns do agree quite well for the angular region covering the first two sidelobes. It is very difficult to make a good comparison for larger angles if we keep the preceding remarks about the measurement in mind.

3.4.3 Fast And Easy Detection Of Defective Elements

If the measured far field radiation pattern of a phased array contains inexplicable deviations from what is expected, then all elements of the phased array would have to be checked. A defective element (or a set of them) might cause this problem. Because the CAISSA antenna consists of 849 radiating elements, this would be a very time consuming process. The near field measurement technique offers an easy and fast method to detect defective elements in a large phased array.

If a large group of elements is defective, then this can be seen immediately from the measured near field amplitude and phase.

Fig 3.4.6 shows an example:

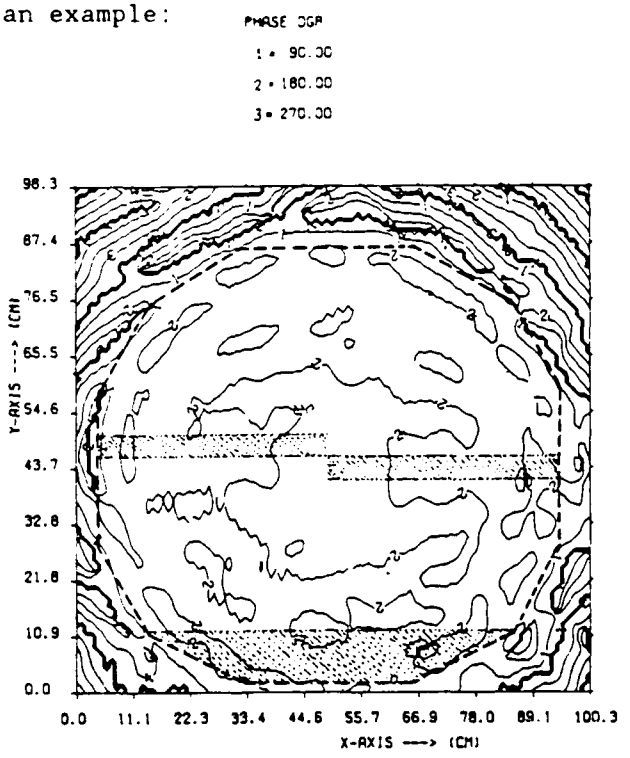

Fig 3.4.6 Contour plot of measured phase of CAISSA with a large group of defective elements

The contour plot of the near field amplitude and phase of the CAISSA antenna with its main beam at broadside should have circular symmetry. This feature is clearly absent in Fig 3.4.6. The power supply of several groups of elements proved to be defective. These groups of elements are shaded in Fig 3.4.6.

If only a few elements are defective, then the following method can be applied: Measure the near field amplitude and phase over the measurement plane for instance for a broadside beam. Calculate with these data the spectrum of this antenna. After this calculate the spectrum back to the aperture-plane of the AUT with an inverse fourier transformation. (Truncate the evanescent waves in this step, because they lead to enormous amplitudes at the aperture plane)

The amplitude and phase distribution at the aperture plane will be found in this way. The phase distribution is shown in Figure 3.4.7:

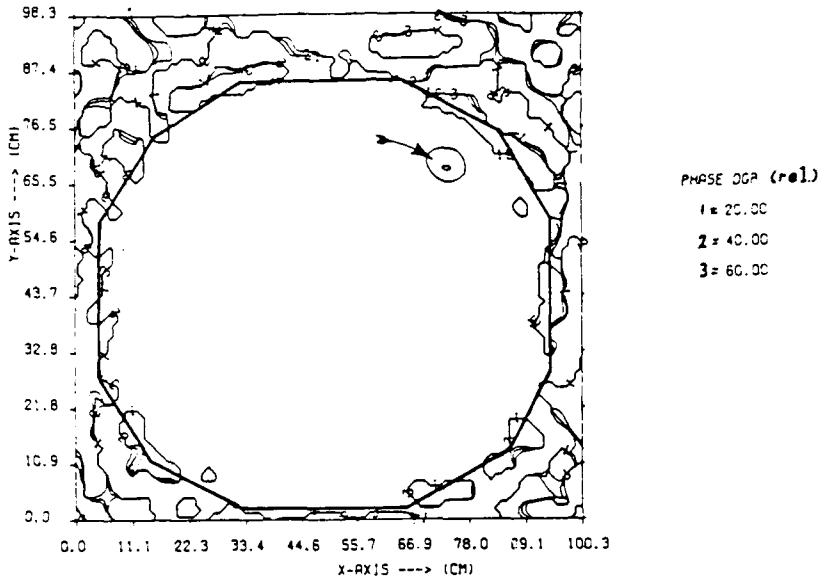

Fig 3.4.7 Detection of defective element with the phase distribution at the aperture plane

The defective element is traced immediately.
Only if a defective element is positioned at the edge of the CAISSA antenna, then it is more difficult to detect (See Fig 3.4.7).
It's of course possible that a phase shifter is defective, but has coincidentally the correct phase so that this phase-shifter would not be noted in this way. To avoid this, perform a second measurement with an additional phase shift of, for instance, 180° for all elements and execute the method again. Then the defective element will appear.[3]

This method can also be applied for other cases:

- Detection of defective elements of an active array:
  Watch both the amplitude and the phase contour at the aperture plane of the AUT
- Positioning of the feed in a parabolic antenna configuration:
  The phase along the aperture of the parabolic reflector should be constant if the feed is placed in the focal point of the reflector.

3.4.4 Difference Patterns

So far, only sum patterns have been considered. Some antennas, like monopulse and tracking antennas, have difference patterns, which contain a sharp minimum (let's say "zero") in the direction, that coincides with the axis of the main beam in the sum pattern.
The exact direction of the "zero", the depth of the "zero" and the pattern just around that "zero" are the parameters of primary interest.
The CAISSA antenna has a monopulse horn and produces a difference pattern in the H-plane (ΔH), which is measured on both the near and far field test range.
The CAISSA antenna is aligned very accurately, such that the "85cm" aperture is placed parallel to the measurement plane within 0.3 mm. So an alignment error of (arctan($\pm$0.3/850)) $\pm$ 0.02° might occur.
The transformation of the near field data to the far field radiation pattern in the φ= 0° or φ=90° plane is mainly a one-dimensional Fourier transformation [5].
An important feature of a Fast Fourier Algorithm is that the number of input values is equal to the number of output values: A limited sequence of 128 measurement points leads to a sequence of calculated far field amplitudes and phases in 128 different directions.

The angular spacing ($\Delta\theta$) between calculated far field radiation points near broadside in the E- or H-plane is given by [3, 5] Eq. 3.4.1:

$$\Delta\theta = \frac{\lambda}{N\delta} \qquad (3.4.1)$$

where λ= wavelength
N= number of points in the calculation in one dimension
δ= sample-spacing in horizontal/vertical direction

For $\delta=0.4\lambda$ and N=128, the obtained angular spacing is $\Delta\theta=1.12°$. This spacing is not sufficient to find accurate information about the parameters of concern, like the depth and the direction of the "zero", and the pattern just around the "zero".
Because the sample spacing satisfies the Nyquist criterion ($\delta \leq 0.5\lambda$), the input array contains all information we need to find the pattern for other angles. We can improve the detail with the well-known 'zero-padding' technique [3, 5] : Zero's are added to the data array (so N increases in Eq (3.4.1))[3, 5] and the angular spacing in the output will be improved correspondingly.
The calculated radiation patterns of the CAISSA antenna, operating in the difference mode, are shown in Fig. 3.4.8 for N=256 and N=8192:

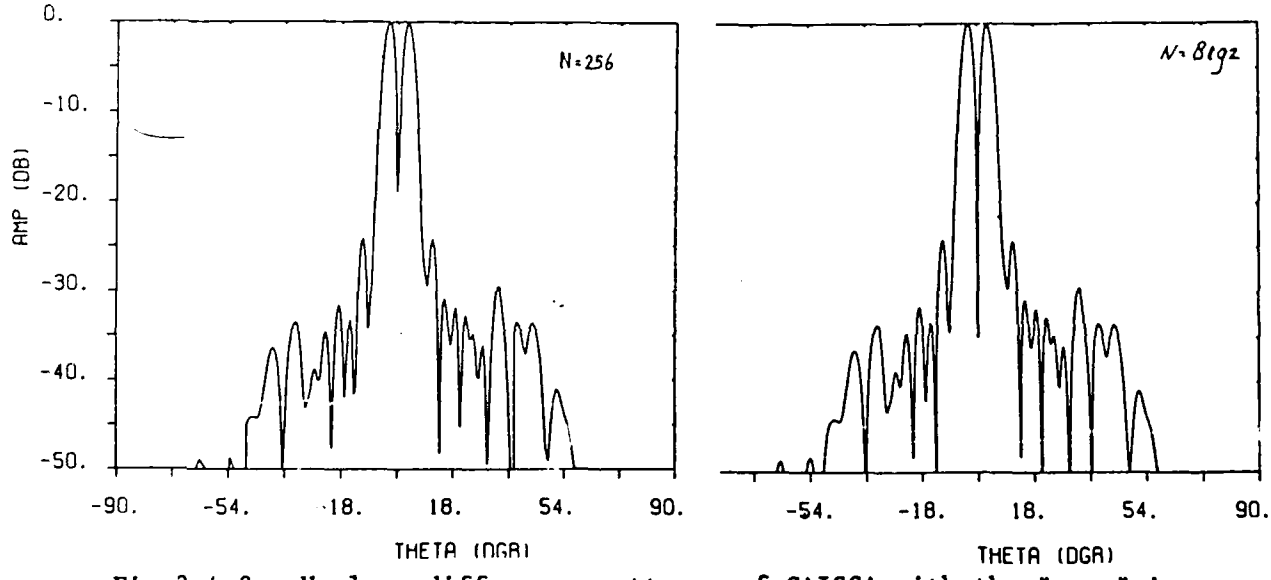

Fig 3.4.8 H-plane difference patterns of CAISSA with the "zero" in broadside as calculated from near field data with N=256 and N=8192 samples in the calculations.(freq=5650 MHz)

The largest difference between these two calculated radiation patterns are at angles around the "zero". The "zero" is deeper for N=8192. The radiation pattern very close to the "zero" contains much more details for N=8192 as we'll see later.
The results for other number of points in the calculation (N) are shown in Table 3.4.1:

N	$\Delta\theta$(°)	depth "zero"(dB)	θ_{zero}(°)
256	0.56	-18.90	0
512	0.28	-27.45	0.28
1024	0.14	-27.83	0.14
2048	0.07	-34.92	0.21
4096	0.035	-34.92	0.21
8192	0.017	-34.92	0.21

Fig. 3.4.1 Important parameters of H-plane difference pattern of CAISSA antenna system obtained from near field measurements as a function of N (freq=5650 MHz)

The depth of the "zero" increases from -18.9 dB(N=256) to -34.92 dB (N≥2048).
The angular spacing ($\Delta\theta$) improves with the number of datapoints used in the calculations according to Eq. (3.4.1).
The direction of the "zero" (θ_{zero}) is obtained when calculations with an improved angular spacing do not deliver a different depth and direction of the "zero". In this case the depth and direction of the "zero" already remained constant for N≥2048.
The exact direction of the zero is now determined with a tolerance equal to the mechanical alignment error.
The near field measurements show a difference between the electric and the mechanical axis of 0.21° ± 0.02°. Far field measurements with accurate information on the direction of the zero are not available, however, because the electrical and mechanical axes have not been determined in measurements [3, p.125].
The subsequent results in the zero region when N is increased from 256 to 8192 points are schwon in Fig. 3.4.9:

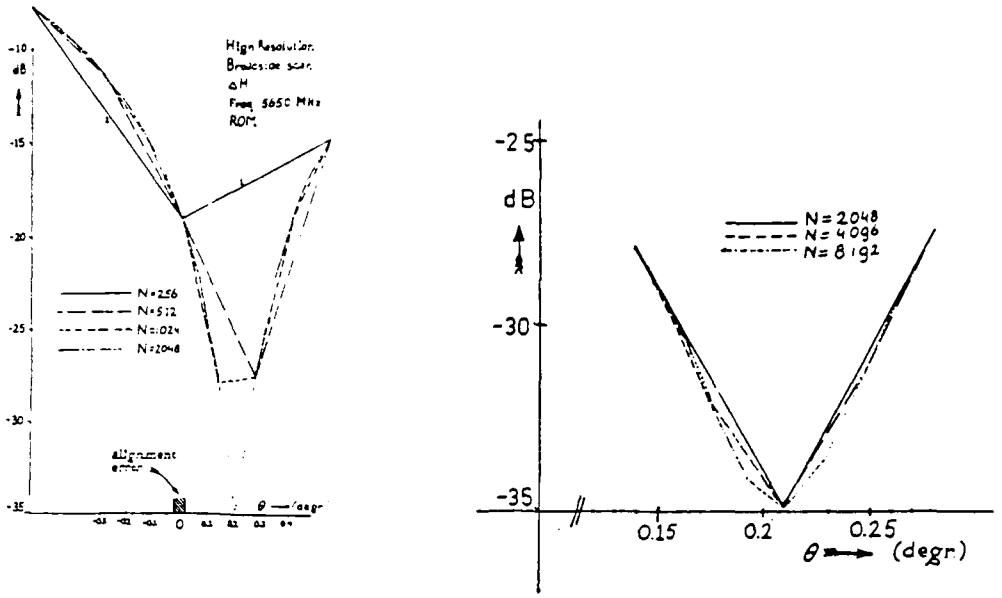

Fig. 3.4.9 Improvement of detail for difference pattern in H-plane of CAISSA antenna around boresight (freq=5650 MHz)

The difference radiation pattern around boresight of the CAISSA antenna in the H-plane, as measured at the FEL-TNO far field test range is shown in Fig 3.4.10:

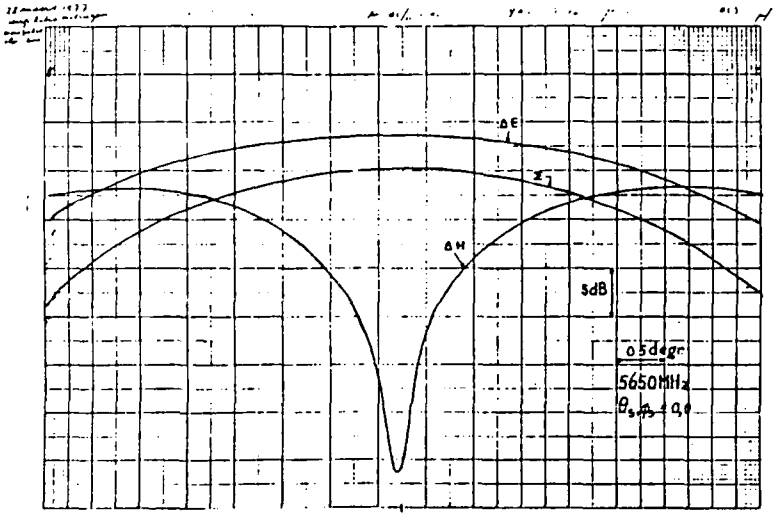

Fig 3.4.10 Difference pattern in H-plane around boresight measured on the far field test range(freq=5650 MHz)

The depth of the "zero" is found to be -30 dB from far field measurements instead of -35 dB from near field measurements. This may be explained by the fact that the electrical and mechanical axes have not been determined, so that not the actual "zero" has been measured. Besides, the far field measurement has been performed a long period earlier than the near field measurements. A change in the CAISSA antenna can have been occurred, because the antenna has been moved and some elements have been replaced.
We may, however, conclude that the FEL-TNO planar near field facility can calculate difference patterns with confidence.

Conclusion

The near field measurement technique offers an easy and fast method to detect defective elements in a large phased array. This method can also be applied to detect defective elements in a large active array and to position the feed in the focal point of a parabolic reflector. Difference patterns can be calculated with confidence from near field measurements. A small angular spacing in the calculated far field patterns is necessary to obtain accurate information about the "depth of the zero", the direction of the "zero" and the pattern around the "zero".

4. CONCLUSIONS

The conclusions of this report are summarized:

The radiation patterns of pencil beam parabolic front fed antennas can be determined with great accuracy with a near field facility. The differences between the calculated and measured far field patterns (about -1 dB at a -30 dB sidelobe level) clearly become larger at lower levels and larger angles θ.

It is possible to measure antennas in a near field facility with aperture dimensions equal or larger than the measurement plane. More than one measurements should be made, with the AUT displaced in the direction in which its aperture dimension is largest. This displacement has to be done very accurately!

Antennas with a far field radiation pattern, which has a small beam in one plane and a broad beam in the other plane, can be calculated with high accuracy in the near field facility. Multiplexing can be applied for pencil-beam antennas to reduce the total near field measurement time, if more patterns of an antenna have to be measured.

The near field measurement technique offers an easy and fast method to detect defective elements in a large phased array. This method can also be applied to detect defective elements in a large active array and to position the feed in the focal point of a parabolic reflector.

Difference patterns can be calculated with confidence from near field measurements. A small angular spacing in the calculated far field patterns is necessary to obtain accurate information about the "depth of the zero", the direction of the "zero" and the pattern around the "zero".

Ir. G.A. van der Spek
(Groupleader)

Ir. J.G. van Hezewijk
(Author)

5. REFERENCES

[1] Collin and Zucker,
"Antenna Theory, part I"
Mc Graw-Hill Book Company, 1969

[2] C.G.M. van 't Klooster and G. Schirinzi
"Planar near-field measurements of a SAR panel"
Internal ESTEC working paper, No. 1449
Noordwijk, The Netherlands, March 1986

[3] C.G.M. van 't Klooster
"De planaire nabije-veld methode voor antenne-metingen"
Physics and electronics laboratory TNO, 1984
Report PHL 1984-22

[4] A.C. Newell,
"Error analysis techniques for planar near field measurements"
IEEE Transactions on Antennas and Propagation,
June 1988, Volume 36, Number 6, p 754-768

[5] A.C. Newell,
"Planar near-field measurements"
Electromagnetic Fields Division of National Bureau of Standards,
Boulder, Colorado, 80303 , June 1985

[6] H.J. van Schaik
"A discussion of the measured radiation patterns of the CAISSA-antenna"
Physics and Electronics Laboratory TNO, 1979
Report PHL 1979-08

REPORT DOCUMENTATION PAGE (MOD-NL)

1. DEFENSE REPORT NUMBER (MOD-NL)	2. RECIPIENT'S ACCESSION NUMBER	3. PERFORMING ORGANIZATION REPORT NUMBER
TD89-4573		FEL-89-B336
4. PROJECT/TASK/WORK UNIT NO.	**5. CONTRACT NUMBER**	**6. REPORT DATE**
710.2	N.A.	NOVEMBER 1989
7. NUMBER OF PAGES	**8. NUMBER OF REFERENCES**	**9. TYPE OF REPORT AND DATES COVERED**
45	6	END REPORT

10. TITLE AND SUBTITLE

MEASUREMENT RESULTS OF THE FEL-TNO PLANAR RECTANGULAR NEAR FIELD FACILITY (1978-1989)

11. AUTHOR(S)

J.G. VAN HEZEWIJK

12. PERFORMING ORGANIZATION NAME(S) AND ADDRESS(ES)

TNO PHYSICS AND ELECTRONICS LABORATORY,
P.O. BOX 96864, 2509 JG THE HAGUE, THE NETHERLANDS

13. SPONSORING/MONITORING AGENCY NAME(S)

14. SUPPLEMENTARY NOTES

15. ABSTRACT (MAXIMUM 200 WORDS, 1044 POSITIONS)

THIS REPORT DESCRIBES THE MOST IMPORTANT RESULTS OF MEASUREMENTS, WHICH HAVE BEEN PERFORMED WITH THE RECTANGULAR PLANAR NEAR-FIELD FACILITY OF THE FEL-TNO LABORATORY FROM 1978 TO 1989.
VARIOUS TYPES OF ANTENNAS HAVE BEEN MEASURED IN THIS PERIOD.
THE RADIATION (BOTH SUM AND DIFFERENCE) PATTERNS OF ANTENNAS WITH NARROW MAIN BEAMS CAN BE DETERMINED WITH GREAT ACCURACY.
THIS IS TRUE AS WELL FOR ANTENNAS, WHICH HAVE DIMENSIONS, THAT ARE EQUAL OR SLIGHTLY LARGER THAN THE MEASUREMENT FRAME OF THE NEAR FIELD SCANNER, OR THAT HAVE A BROAD MAIN BEAM IN ONE PLANE.
BESIDES, THE NEAR FIELD MEASUREMENT FACILITY OFFERS THE POSSIBILITY TO DETECT DEFECTIVE RADIATING ELEMENTS IN A LARGE ARRAY ANTENNA VERY FAST.
IF A PARAMETER, LIKE THE FREQUENCY OR THE SCAN-DIRECTION OF THE MAIN BEAM, CAN BE CHANGED VERY QUICKLY, THEN WE CAN DETERMINE MORE RADIATION PATTERNS OF AN ANTENNA DURING THE TIME NEEDED TO PERFORM ONE SINGLE NEAR FIELD MEASUREMENT.
THE REPORTED MEASUREMENTS GIVE A GOOD OVERVIEW OF THE POSSIBILITIES OF THE PLANAR NEAR FIELD MEASUREMENT TECHNIQUE.

16. DESCRIPTORS	IDENTIFIERS
RADAR	NEAR FIELD
ANTENNA	
ANTENNA TEST	
MEASURING OF ELECTROMAGNETIC FIELD	

17a. SECURITY CLASSIFICATION (OF REPORT)	17b. SECURITY CLASSIFICATION (OF PAGE)	17c. SECURITY CLASSIFICATION (OF ABSTRACT)
UNCLASSIFIED	UNCLASSIFIED	UNCLASSIFIED

18. DISTRIBUTION/AVAILABILITY STATEMENT	17d. SECURITY CLASSIFICATION (OF TITLES)
UNLIMITED AVAILABILITY	UNCLASSIFIED